Influence of heterostructure on electron localization in the CdTe/ZnTe/CdTe spherical core-shell quantum antidot with hydrogenic impurity in the center

D. STOJANOVIĆ*, R. KOSTIĆ
University of Belgrade, Institute of Physics, PO Box 68 11080 Belgrade, Serbia

Calculations of the hydrogenic impurity discrete states in the partially closed spherical semiconductor core-shell quantum antidot (QAD) are performed under effective mass approximation. On the basis of the analytical solutions of the Scrödinger and Poisson equations for multilayered quantum antidot (MLQAD) with hydrogenic impurity located in the center, energies of an electron bound states in closed part of potential and corresponding wave functions are determined. Particular core/shell/surrounding medium nanoheterosystem under investigation is CdTe/ZnTe/CdTe MLQAD. ZnTe shell forms potential barrier. The influence of increasing core and shell size on the ground state (1s) energy and corresponding radial probabilities are presented in this paper. For small core radius 1s orbital expands out of the shell with energy just below the bottom of the outer material conduction band i.e. core material in this particular case. When core radius increases, at characteristic radius value, 1s orbital contracts into the core region and the ground state energy decreases. For very large core radius, energy of 1s state reaches constant value, characteristic for bulk core material.

1. Introduction

Low-dimensional structures doped by hydrogenic impurity change their optical, electrical and thermal properties. In last few years, hydrogenic impurity confined in QD [1-5], multi-layered quantum dot (MLQD) [5-10] or quantum antidots (QAD) [11-15] have been investigated intensively. Results of these investigations explain how the presence of hydrogenic impurity influences on properties of different heteronanostructures.

The most investigations deal with so called "closed" nanostructures, with stationary electron states [1-10]. There is increasing interest for "opened" systems [8, 11-15]. If there is potential barrier in heterostructure, compared to the potential of surrounding space, the system is opened. We denote potential of surrounding space as $V(\infty)$. In energy region $E > V(\infty)$ spectrum is characterized by quasistationary states and in energy region $E < V(\infty)$ discrete spectrum of bound states is formed. Nanoheterostructure CdTe/ZnTe/CdTe is an example of such a structure. In the absence of hydrogenic impurity it is an opened QD: $V(r) \geq V(\infty)$ with quasistationary states [16,17]. Presence of hydrogenic impurity in the system produces potential $V(r) < V(\infty)$ in some regions of the QD, and consequently formation of bound states with energy $E < V(\infty)$.

In this paper we deal with the "opened" system but only in the energy region of bound states. We present results of calculation of one-electron opened multi-layered spherical QAD. QAD consists of CdTe spherical core coated by spherical ZnTe shell i.e. potential barrier, surrounded by bulk CdTe with a hydrogenic impurity in the center.

2. Theory and calculations

Investigated semiconductor MLQAD can be described as a system composed of an electron and a positively charged donor impurity located at the centre of the multilayered spherical potential (D⁰). A single MLQAD is considered. The validity of the effective mass approximation is assumed. Difference of the electron effective masses and dielectric constants between QD regions are considered.

The stationary Schrödinger equation for D⁰ in the effective mass approximation, considering that electron spectra is mainly formed by size quantization, has the form

$$\left(-\frac{\hbar^2}{2}\nabla\frac{1}{m^*(r)}\nabla + W(r) + U(r)\right)\Psi(r) = E\Psi(r). \quad (1)$$

$$m^*(r) = \begin{cases} m_1^* & r \leq r_1, \\ m_2^* & r_1 < r \leq r_2 \ . \\ m_3^* & r > r_2 \end{cases} \quad (2)$$

is the effective mass of an electron in the heterosystem.

The potential energy of interaction of an electron with positively charged ion located at the center of spherical MLQD is solution of Poisson equation and has the form [15]

$$W(r) = -\frac{Ze^2}{4\pi} \begin{cases} \dfrac{\varepsilon_1 - \varepsilon_2}{\varepsilon_1 \varepsilon_2 r_1} + \dfrac{1}{\varepsilon_1 r} + \dfrac{\varepsilon_2 - \varepsilon_3}{\varepsilon_3 \varepsilon_2 r_2} & r \leq r_1 \\[3mm] \dfrac{1}{\varepsilon_2 r} + \dfrac{\varepsilon_2 - \varepsilon_3}{\varepsilon_3 \varepsilon_2 r_2} & r_1 < r \leq r_2 \\[3mm] \dfrac{1}{\varepsilon_3 r} & r > r_2 \end{cases} \quad (3)$$

We examined case $Z = 1$ i.e. hydrogen like impurity. The confinement potential is

$$U(r) = \begin{cases} -U_0 & r \leq r_1 \\ 0 & r_1 < r \leq r_2 \quad U_0 > 0 \\ -U_0 & r > r_2 \end{cases} \quad (4)$$

We assigned a potential energy as zero on the top of the barrier. U_0 is barrier height. ε_i are the corresponding static dielectric constants. In energy scale assumed in this manner $V(\infty) = W(\infty) + U(\infty) = -U_0$. The barrier width, $r_2 - r_1$, is assigned as Δ. Scheme of the potential energy, on the basis of relations (3) and (4), for particular structure examined in this paper, at $r_1 = 2$ nm and $\Delta = 2$ nm is presented in Fig. 1.
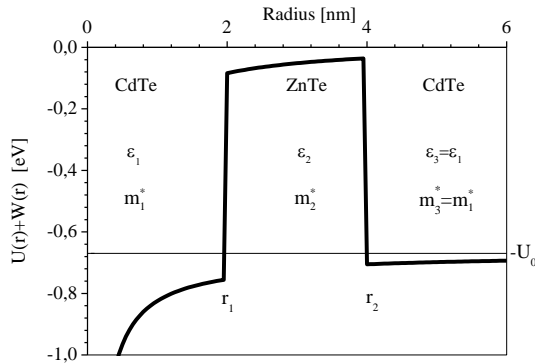
Fig. 1. Potential energy $U(r)+W(r)$ at $r_1 = 2$ nm and $\Delta = 2$ nm.

Without impurity, $Z = 0$, it is an example of opened spherical MLQD. There are no bound states. In energy region $E > -U_0$ there are quasi stationary states [16, 17]. In the presence of hydrogenic impurity in the center, Coulomb potential produces two potential wells: the deep one inside the core ($r < r_1$) and shallow one outside the barrier ($r > r_2$). This enables existence of bound states in energy region $E < -U_0$, i.e. below conductive band core energy. In this paper we investigate bound states i.e. states in energy region $E < -U_0$. Composition in which electron is localized outside the barrier is usually assigned as quantum antidot.

For spherically symmetric potential, $U(r)$ and $W(r)$, the separation of radial and angular coordinates leads to:

$$\Psi_{lm}(r) = R_l(r) Y_{lm}(\theta, \varphi). \quad (5)$$

$R_l(r)$ is the radial wave function, and $Y_{lm}(\theta,\varphi)$ is a spherical harmonic. The differential equation for the radial function $R_l(r)$ can be written as:

$$-\frac{\hbar^2}{2m^*(r)} \left(\frac{\partial^2}{\partial r^2} + \frac{2}{r}\frac{\partial}{\partial r} - \frac{l(l+1)}{r^2} \right) R_l(r) + (W(r) + U(r)) R_l(r) = E R_l(r) \quad (6)$$

The radial function $R_l(r)$, consist of three parts, because it spreads through three different regions:

$$R_l = \begin{cases} R_l^1 & r \leq r_1 \\ R_l^2 & r_1 < r \leq r_2 \\ R_l^3 & r > r_2 \end{cases} \quad (7)$$

Solutions must satisfy conditions $R_l(r)$ to be regular when $r = 0$ and to vanish sufficiently rapidly when $r \to \infty$.

In spherical MLQD with impurity, differential equation (6) concerns to all, separated, QD regions. Problem has analytical solutions. In each QD region there are two energy regions, where equation (6) transforms to different equations with corresponding analytical solutions. We assigned that characteristic energy off each QD region as U_i^*. It is the depth of effective potential well. In the system under investigation there are three geometry regions: $r \leq r_1$, $r_1 < r \leq r_2$ and $r > r_2$. Effective potential is defined as:

$$U_i^*(r_1, r_2) = \begin{cases} \dfrac{Ze^2}{4\pi}\dfrac{\varepsilon_1 - \varepsilon_2}{\varepsilon_1 \varepsilon_2 r_1} + \dfrac{Ze^2}{4\pi}\dfrac{\varepsilon_2 - \varepsilon_3}{\varepsilon_3 \varepsilon_2 r_2} + U_0 & r \leq r_1 \\[3mm] \dfrac{Ze^2}{4\pi}\dfrac{\varepsilon_2 - \varepsilon_3}{\varepsilon_3 \varepsilon_2 r_2} & r_1 < r \leq r_2 \\[3mm] U_0 & r > r_2 \end{cases}$$
$$Z = 1 \quad (8)$$

$i = 1$, 2 and 3 correspond to regions $r \leq r_1$, $r_1 < r \leq r_2$ and $r > r_2$, respectively. Effective potentials depend on dimensions in heterostructure and the dielectric permittivities. In a system where: $\varepsilon_1 = \varepsilon_3 > \varepsilon_2$, only effective potential $-U_1^*$, characteristic for core region belongs to energy region $E < -U_0$. In energy region $E < -U_1^*$ conditions $E < -U_2^*$ and $E < -U_3^*$ are already fulfilled.

For energy range $E < -U_1^*$, introducing convenient parameters: $\alpha_i^2 = -8m_i^*(E + U_i^*)/\hbar^2$, $\xi_i = \alpha_i r$, $\lambda_i = 2m_i^* e^2/4\pi\varepsilon_i \hbar^2 \alpha_i$, $R^i(\xi_i) = \xi_i^{-1}\chi(\xi_i)$, the radial Schrödinger equation becomes:

$$\frac{\partial^2 \chi}{\partial \xi_i^2} + \left[-\frac{1}{4} + \frac{\lambda_i}{\xi_i} + \frac{\frac{1}{4} - (l + \frac{1}{2})^2}{\xi_i^2} \right]\chi = 0. \quad (9)$$

Equation (9) is the Whittaker equation with two linearly independent solutions and the radial wave functions in three regions are:

$$R_i^i(\alpha_{1a}r) = C_{1i}\frac{1}{\xi_i}M(\lambda_i, l+\frac{1}{2}, \alpha_i r) + C_{2i}\frac{1}{\xi_i}W(\lambda_i, l+\frac{1}{2}, \alpha_i r),$$

$$i = 1, 2, 3. \qquad (10)$$

C_{1i} and C_{2i} are the normalization constants, M and W are Whittaker functions. For $C_{21} = 0$ assumed solutions satisfy conditions to be regular at $r = 0$ and $C_{13} = 0$ to vanish sufficiently rapidly when $r \to \infty$.

For energy range $-U_1^* < E < -U_0$, introducing parameters for $i = 1$, $r < r_1$, $\alpha_{1b}^2 = 2m_1^*(E+U_0)/\hbar^2 > 0$, $\xi_1 = \alpha_{1b}r$, $\beta_1 = -m_1^*e^2/4\pi\varepsilon_1\hbar^2\alpha_{1b}$, $R(\xi_1) = \xi_1^{-1}F(\xi_1)$, equation (6) becomes:

$$\frac{\partial^2 F}{\partial \xi_1^2} + \left[1 - \frac{2\beta_1}{\xi_1} - \frac{l(l+1)}{\xi_1^2}\right]F = 0. \qquad (11)$$

Equation (11) is the Coulomb equation which have two linearly independent solutions $F_{\beta_1,l}(\xi_1)$ and $G_{\beta_1,l}(\xi_1)$. $G_{\beta_1,l}(\xi_1)$ is a singular at $\xi_1 = 0$, hence the wave function of the radial part is expressed as:

$$R_l^1(\alpha_{1b}r) = C_{1b}\frac{1}{\xi}F_{\beta_1,l}(\xi_1). \qquad (12)$$

C_{1b} is the normalization constant. The regular Coulomb wave function $F_{\beta1,l}(\zeta_1)$ is defined in the following way:

$$F_{\beta_1,l}(\xi_1) = AM(i\beta_1, l+\frac{1}{2}, 2i\xi_1) \qquad (13)$$

where:

$$A = \frac{|\Gamma(l+1+i\beta_1)|\exp[-\pi\beta_1/2 - (l+1)\pi i/2]}{2(2l+1)!}. \qquad (14)$$

M and Γ are Whittaker and Gamma functions. In relations (13) and (14) i is imaginary number.

For energy range $-U_1^* < E < -U_0$, and radius regions $r_1 < r \le r_2$ ($i = 2$) and $r > r_2$ ($i = 3$), conditions $E < -U_2^*$ and $E < -U_3^*$ are already fulfilled, equation (6) transforms to Wittaker equation (9), that leads to already described solutions.

The wave functions and the probability current at the boundary of the layers of the system must satisfy continuity conditions. This leads to the system of linear equations characteristic for each l. Solutions of this system are eigenenergies E_{nl}. Solutions are numerated by n in the order of increasing energy. Among all states, the lowest energy solution is $l = 0$, $n = 1$ i.e. it is ground state ($1s$). After normalization, corresponding radial part of wave function $R_{nl}(r)$ is determined.

3. Results and discussion

Method presented in previous section is used for investigation of heterostructure that consists of CdTe core (1), ZnTe barrier (2) and CdTe surrounding material (3).

We have used the material parameters $m_{e1}^* = m_{e3}^* = m_{CdTe}^* = 0.099m_e$, $m_{e2}^* = m_{ZnTe}^* = 0.116m_e$, $\varepsilon_{r1} = \varepsilon_{r3} = \varepsilon_{rCdTe} = 10.2$, $\varepsilon_{r2} = \varepsilon_{rZnTe} = 7.4$, $U_1 = 0.67$ eV. The effective Bohr radius of material, defined as $a_B^* = \hbar^2 4\pi\varepsilon/m_e^* e^2$, is often used as the unit of the length. For examined materials: $a_{B1}^* \approx 5.4$ nm for CdTe and $a_{B2}^* \approx 3.376$ nm for ZnTe. The effective Rydberg of material, defined as $Ry^* = m^* e^4/2\hbar^2(4\pi)^2\varepsilon^2$, can be used as unit of the energy. In this case $Ry_1^* = Ry_3^* \approx 13.06$ meV for CdTe and $Ry_2^* \approx 28.82$ meV for ZnTe.

In the examined structure, there are two geometry parameters that determine structure of the QD: core radius r_1 and outer dot radius r_2 or barrier width $\Delta = r_2 - r_1$. As can be seen from relations (3) and (4) and presentation in Fig. 1. three characteristic potential regions can be separated: $r < r_1$ is region of deep potential well in CdTe core; $r_1 < r < r_2 = r_1 + \Delta$ region of potential barrier in ZnTe shell and region $r > r_2$ of shallow well outside the dot i.e. in the surrounding CdTe. Outer radius is a shallow well distance from the dot center. Depth of the shallow well outside the dot depends only on the outer dot radius and dielectric permittivity: ε_3 ($\varepsilon_1 = \varepsilon_3$). Depth of the shallow well is $\sim 1/(r_2 \varepsilon_3)$. Outer radius increase produces the shallow well depth decrease.

Results of calculated energies for ground state, first solution for orbital quantum number $l = 0$ i.e. 1s state, for increasing core radius r_1 from 0 to 60 nm ≈ 11 a_{B1}^* and four different barrier widths Δ (1 nm, 5 nm, 10 nm and 50 nm) are presented in Fig. 2. With the increase of the core radius r_1 for constant barrier thickness Δ, outer dot radius r_2 increases.
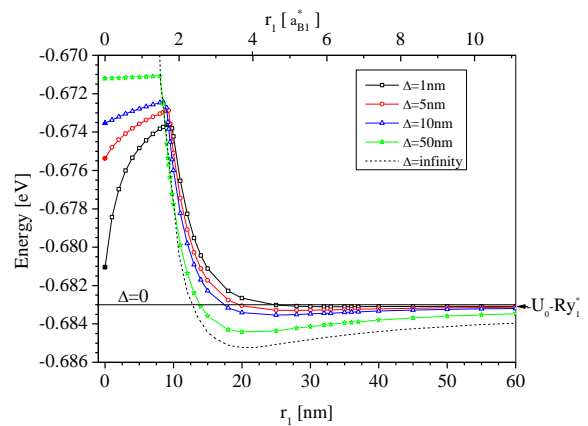
Fig. 2. One electron ground state energy in spherical CdTe/ZnTe/CdTe QD with hydrogen impurity in the center as function of core radius r_1, ($Z = 1$, $l = 0$, $n = 1$) for four different barrier widths $\Delta = 1$ nm, 5 nm, 10 nm and 50 nm.

We start analysis of results for small core radius. Calculated energies for QAD of $r_1 = 0$ are added as points

at the beginning of each curve as solid symbol of the same shape as the rest of the curve. Results for small core radius r_1, Fig. 2. practically reach values of $r_1 = 0$ case. In Fig. 2. we present results for four different barrier widths only. To complete the picture about system behavior for case $r_1= 0$, $r_2= \Delta$ we present results separately in Fig. 3.

For $r_1 = 0$ this multilayered QD becomes QAD, with material of higher potential (ZnTe) in the center that forms core of radius $r_2 = \Delta$. Calculated energies are presented in Fig. 3. Potential scheme of $r_1 = 0$, $r_2 = \Delta = 10$ nm case is presented in the insert in Fig. 3. Slope of the potential curve in core region disables to see potential well in the core. Deep potential well is close to the center of the dot. Probability density spreads from $r = \Delta = 10$ nm till few tenths nm with maximum in probability density at ≈ 25 nm $\approx 4.6\, a_{B1}^{*}$. For small ZnTe core dimension ($r_2 = \Delta$), space of the deep well is in small radius region close to the center. This unables electron to locate in the core i.e. space of this deep potential well. Electron is pushed out of ZnTe core into the shallow well formed by Coulomb potential in the surrounding CdTe. As Δ increases (Δ is now ZnTe core radius), distance of the shallow well, out of the dot, from the center increases, depth of the shallow well decreases and electron energy increases. This increase in energy is a sign that electron is forced to stay in a shallow well out of the dot, despite the fact of increasing dimension of the core. If $U_0 > Ry_2^{*}$ (as in this case: 670 meV $>>$28.82 meV) electron will stay in shallow well for any dimension of core. If the barrier height U_0 is smaller than Ry_2^{*} ($U_0 <Ry_2^{*}$), for large enough core radius electron would move into the core and energy would decrease. In the limiting case when $\Delta = 0$ ($r_1 = 0$, $r_2 = r_1+\Delta = 0$, there is no barrier) electron is in potential of hydrogenic impurity in CdTe, characterized by m_{CdTe}^{*} and ε_{rCdTe} and has energy characteristic for 1s state: $E_{1s}=-U_0-Ry_1^{*}\approx-683$ meV, starting point in Fig. 3, with maximum in probability density at $\approx 1\, a_{B1}^{*}$.
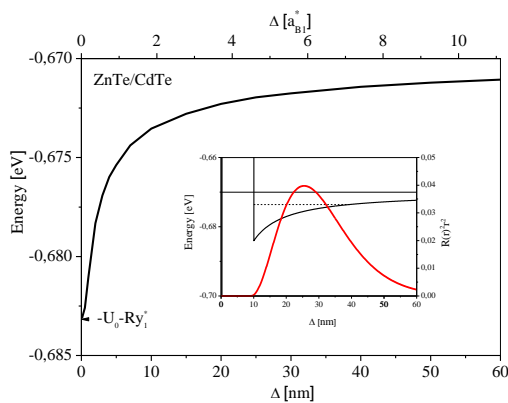
Fig. 3. One electron ground state energy in spherical ZnTe/CdTe QAD ($r_1 = 0$) with hydrogen impurity in the center as function of dot radius $r_2 = \Delta$ ($Z = 1$, $l = 0$, $n = 1$).

When core radius ($r_1 \neq 0$) increases from 0 up to ≈ 10 nm $\approx 2\, a_{B1}^{*}$, electron energy increases for any Δ, Fig. 2. This increase is a sign that electron is in the region of shallow well out of the dot. To illustrate properties of this

system we present potential scheme and radial probability density for few characteristic compositions, Fig. 4. and Fig. 5. In Fig. 4. we present potential scheme and radial probability density for barrier thickness $\Delta = 5$ nm. In Fig. 4.a) $r_1= 5$ nm $< 1\, a_{B1}^{*}$, $r_2 = 10$ nm. Electron is in the shallow well in the surrounding CdTe region, $E_{1s} =-673$ meV. Electron spreads up to 60 nm with maximum of the probability density at $r \approx 25$ nm $\approx 4.6\, a_{B1}^{*}$. Also, in Fig. 5.a) we present potential scheme and radial probability density for $\Delta = 10$ nm and core radius $r_1 = 8$ nm $\approx 1.5\, a_{B1}^{*}$ i.e. $r_2 = 18$ nm $\approx 3.3\, a_{B1}^{*}$. Curve E_{1s} for $\Delta = 10$ nm reaches maximum at $r_1^{max} = 8.5$ nm $\approx 1.6\, a_{B1}^{*}$, Fig. 2, and core radius of 8 nm is close to this value. Electron is in the shallow well and spreads up to 100 nm. Maximum of the probability density is at $r \approx 40$ nm $\approx 7.4\, a_{B1}^{*}$.

While electron is in the shallow well, among dots of same core radius (r_1), dots of smaller barrier thickness (Δ) i.e. smaller QAD radius ($r_2 = r_1+\Delta$), have deeper shallow well in radius region closer to the center of the dot and consequently smaller electron energy, Fig 2. E_{1s} ($\Delta = 1$ nm) $< E_{1s}$ ($\Delta = 5$ nm)$< E_{1s}$ ($\Delta = 10$ nm)$<...< E_{1s}$ ($\Delta = 50$ nm). This behavior is a sign that electron is in the region of shallow well.
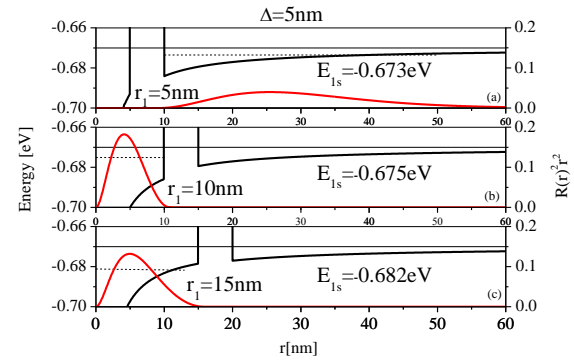
Fig. 4. Potential scheme and ground state radial probability distribution for $\Delta = 5$ nm and different r_1 a) $r_1 = 5$ nm $< 1\, a_{B1}^{*}$, b) $r_1 = 10$ nm $\approx 1.85\, a_{B1}^{*}$ and c) $r_1 = 15$ nm $\approx 2.78\, a_{B1}^{*}$. The energies of the levels are shown by the dashed lines.
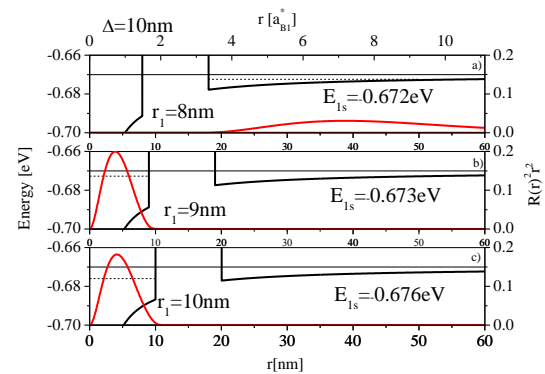
Fig. 5. Potential scheme and ground state radial probability distribution for $\Delta = 10$ nm and different r_1 a) $r_1 = 8$ nm $\approx 1.48\, a_{B1}^{*}$, b) $r_1 = 9$ nm $\approx 1.67\, a_{B1}^{*}$ and c) $r_1 = 10$ nm $\approx 1.85\, a_{B1}^{*}$. The energies of the levels are shown by the dashed lines.

Energy increase slows down and from characteristic core radius electron energy rapidly decreases for all Δ. Core radius at which electron energy reaches maximum and than rapidly decreases (r_1^{max}) does not depend on the Δ value too much. For instance: for $\Delta = 5$ nm $r_1^{max} \approx 9$ nm $\approx 1.67\ a_{B1}^*$, for $\Delta = 10$ nm $r_1^{max} \approx 8.5$ nm $\approx 1.57\ a_{B1}^*$ and for $\Delta = 50$ nm $r_1^{max} \approx 8$ nm $\approx 1.48\ a_{B1}^*$, Fig. 2. Energy decrease is a sign that the dimension of the core is big enough and electron moves into the core region i.e. region of deep potential well. Potential scheme and radial probability density presented in Fig. 5. a) and b) illustrate that. For core radius $r_1 = 8$ nm $\approx 1.48\ a_{B1}^*$ and $\Delta = 10$ nm, Fig. 5. a), electron is completely in radius region $r > r_2 = r_1 + \Delta$, but for $r_1 = 9$ nm $\approx 1.67\ a_{B1}^*$ and $\Delta = 10$ nm electron is completely in the core, Fig. 5. b). Maximum in radial probability density is at $r \approx 4$ nm $\approx 0.74\ a_{B1}^*$. For these two very similar compositions, electron is located in different part of the heterosystem. This drastic change in electron position is followed by minimal change in energy because we are in the vicinity of $r_1^{max}(\Delta = 10$ nm$) \approx 8.5$ nm $\approx 1.57\ a_{B1}^*$. If the core radius further increase just for 1 nm we get $r_1 = 10$ nm $\approx 1.85\ a_{B1}^*$, Fig. 5. c). Electron stays in the deep well in the core CdTe region, energy decreases: $E_{1s} = -676$ meV.

Core radius region of drastic energy decrease is characterized with electron localized in the core but drastically confined. Core radius increase from 8 nm to 15 nm produces drastic decrease in energy. When the core radius becomes big enough, electron will be situated in the next manner: maximum of radial probability density at $r \approx 5.4$ nm $\approx 1\ a_{B1}^*$ and energy $E \approx -U_1^* - Ry_1^*$. Typical core radius values from region of drastic energy decrease are presented in Figs. 4. b), c) and 5. c). In Fig. 4. b) $r_1 = 10$ nm $\approx 1.85\ a_{B1}^*$, $\Delta = 5$ nm. Electron is in the deep well in the core CdTe region. Maximum of the probability density is at $r \approx 4$ nm $\approx 0.74\ a_{B1}^*$. Electron energy is $E_{1s} = -675$ meV. Further increase in core radius leads to situation presented in Fig. 4. c) where $r_1 = 15$ nm $\approx 2.78\ a_{B1}^*$, $\Delta = 5$ nm. Electron is in the deep well in the core CdTe region, $E_{1s} = -682$ meV, still much above $-U_1^* - Ry_1^*$, and maximum of the probability density is at $r \approx 4.5$ nm $\approx 0.83\ a_{B1}^*$.

As the core radius further increases, this rapid decrease in energy slows down for all Δ and electron energy goes below $-U_0 - Ry_1^*$ value. Electron energy stabilizes for core radius $r_1 > 20$ nm $\approx 3.7\ a_{B1}^*$, Fig. 2. Electron is localized in the core. It is in the Coulomb potential and has stabilized energy and probability density. Increase of core dimension does not influence on electron energy because size confinement does not play any role. There is a minimum in energy of 1s state: for $\Delta = 10$ nm at core radius $r_1^{min} \approx 25$ nm $\approx 4.6\ a_{B1}^*$, for $\Delta = 5$ nm at core radius $r_1^{min} \approx 30$ nm $\approx 5.55\ a_{B1}^*$ and for $\Delta = 1$ nm at core radius $r_1 \approx 40$ nm $\approx 7.4\ a_{B1}^*$. This minimum is characterized by energy $-U_1^*(r_1, \Delta) - Ry_1^*$. Electron is in the core with maximum probability density close to $r \approx 1\ a_{B1}^*$, but in potential $-U_1^*(r_1, \Delta)$ resulting in energy $-Ry_1^*$ below $-U_1^*$. The wider the barrier the lower is $-U_1^*$.

That is why in case of the same core radius and wider barrier, energies are lower and minimum is more prominent. Minimum in energy is consequence of the already described approach. Potential energy of interaction of an electron with ion is solution of Poisson equation, equation (3), and consequently can be presented through effective potential, equation (8). Materials of core, barrier and surrounding medium are introduced as different dielectrics. Value of $-U_1^*$ also depends on the dielectric properties of core, shell and surrounding materials: ε_1, ε_2 and ε_3. In the examined structure $\varepsilon_1 = \varepsilon_3$. For higher ε_1 and smaller ε_2, $-U_1^*$ and consequently $-U_1^* - Ry_1^*$ will be lower in energy scale. Result is that minimums are at lower energy. If $\varepsilon_1 = \varepsilon_2 = \varepsilon_3$ i.e. $\varepsilon_1 - \varepsilon_2 = \varepsilon_2 - \varepsilon_3 = 0$, than $-U_1^* = -U_0$, $-U_2^* = 0$ and $-U_3^* = -U_0$, there will be no minimum in energetic spectra.

After minimum, energy slowly increases and stabilizes. This slow increase is consequence of slow increasing effective potential $-U_1^*$. Energies are $\sim -U_1^*(r_1, \Delta) - Ry_1^*$. Electron energy is lower for wider barrier, Fig.2.

This stabilized energy is a sign that electron is completely in the core with maximum probability density at $r \approx 1\ a_{B1}^* \approx 5.4$ nm, and electron is not very sensitive to the change in core or barrier dimension any more.

In the region $r_1 > r_1^{max}$ in the limit: $\Delta \to \infty$ i.e. $r_2 \to \infty$, electron behaves as it is in potential of hydrogenic impurity in closed CdTe/ZnTe QD. Solutions for the closed CdTe/ZnTe QD [18] in region below core material (CdTe) conduction band are presented in Fig. 2. by dashed line and assigned as $\Delta \to \infty$. This is the limit of the thickest barrier. That is why $\Delta \to \infty$ (dashed line) curve is the lowest one in core radius region $r_1 > 9$ nm $\approx 1.6\ a_{B1}^*$, with the most prominent minimum located at $r_1^{min} \approx 20$ nm $\approx 3.5\ a_{B1}^*$, Fig. 2. As we can see from Fig. 2., energy maximums for different Δ, positioned at r_1^{max}, are practically on the dashed curve ($\Delta \to \infty$). This is core-shell composition when electron starts to move from outer shallow well to the core.

In the limit: $r_1 \to \infty$, electron behaves as it is in potential of hydrogenic impurity in CdTe and $E_{1s} \to -U_0 - Ry_1^* \approx -683$ meV (horizontal line at Fig. 2). This is almost achieved for the largest core radius presented in Fig. 2. The same value of energy is achieved for any radius r_1 in limiting case $\Delta = 0$.

Results presented in Figs. 2. and 3. are in accordance with the results of other authors where opened MLQAD [15] and QAD [11-14] were investigated.

4. Conclusion

Energies of ground state of CdTe/ZnTe/CdTe QAD in presence of hydrogenic impurity within effective mass approximation are calculated and presented. Presence of hydrogenic impurity changes "open" structure to partially "closed". On the basis of exact solution of Poisson equation for this system we introduced effective potential for electron in the heterostructure. Consideration of the exact solution of the Poisson equation allows us to reveal

the presence of a minimum in the ground state energy spectra.

For small core radius electron is forced to stay in a shallow potential well out of the barrier. Depth of the shallow well depends on the QAD radius and dielectric permittivity in surrounding medium. Shallow well is deeper for smaller QAD and small ε_2. Electron energy increase as QAD radius increases.

From characteristic core radius electron abruptly moves to the core i.e. region of deep potential well. This transition is followed by drastic decrease in energy till the minimum. Depth of deep well depends on the structure and dielectric properties. Potential well is deeper for higher ε_1 value and lower ε_2. For large core radius electron energy becomes stabilized ($E \sim -U_0 - Ry_1^*$) as if system is closed spherical CdTe/ZnTe QD. For large core radius electron is located in deep potential well in the core with maximum probability density at $\approx 1\, a_{B1}^*$. It is obvious that higher barrier more efficiently prevent penetration from the surrounding to the core with the core radius increase.

Results presented in this paper concerns to MLQAD formed by CdTe and ZnTe, widely investigated constituents in nanoheterostructures, but these results give information on the nature of the impurity states in MLQADs.

Acknowledgment

References

[1] C- Y. Hsieh, D. S. Chuu, J. Phys: Condens. Matter **12**, 8641 (2000).

[2] M. C. Lin, D. S. Chuu, J. Appl. Physics **90**, 2886 (2001).

[3] M. Sahin, Phys. Rev. B **77**, 045317 (2008).

[4] D. Stojanović, R. Kostić, Acta Physica Polonica A **120**, 234 (2011).

[5] A. Ozmen, B. Cakir, Y. Yakar, Journal of Luminescence **137**, 259 (2013).

[6] M. Cristea, E. C. Niculescu, Eur. Jour. Phys. B **85**, 191 (2012).

[7] E. C. Niculescu, M. Cristea, Journal of Luminescence **135**, 120 (2013).

[8] A. R. Jafari, Y. J. Naimi, Comput. Electron. **12**, 36 (2013).

[9] V. Holovatsky, O. Makhanets, I. Frankiv, Rom. Jour. Phys. **57**(9-10), 1285 (2012).

[10] H. Has, M. Sahin, J. Appl. Phys. **112**, 053717 (2012).

[11] V. I. Boichuk, I. V. Bilynskyi, R. Ya. Leshko, L.Ya. Voronyak, Ukr. J. Phys. **54**(10), 1021 (2009).

[12] R. Khordad, N. Fathizadeh, S. Davatolhagh, A. R. Jafari, Eur. Phys. J. B **85**, 353 (2012).

[13] Y. Naimi, Physica B **42**, 43 (2013).

[14] V. Holovatsky, O. M. Makhanets, O. V. Voitsekhivska, Physica E **41**, 1522 (2009).

[15] V. I. Boichuk, I. V. Bilynskyi, R. Ya. Leshko, L. Ya. Voronyak, J. Phys. Studies **14**(1), 1702 (2010).

[16] N. V. Tkach, Yu. A. Seti, G. G. Zegrya, Technical Physics Letters **33**(1), 35 (2007).

[17] D. Stojanović, R. Kostić, Acta Physica Polonica A **117**, 768 (2010).

_____

[*]Corresponding author: dusanka@ipb.ac.rs